LBL-33355
UC-410

Lawrence Berkeley Laboratory

UNIVERSITY OF CALIFORNIA

Accelerator & Fusion Research Division

Presented at the SPIE 1993 International Symposium on Optical Applied Science and Engineering, San Diego, CA, July 11–16, 1993, and to be published in the Proceedings

Monte Carlo Calculation of Multi-Electron Effects on Synchrotron Radiation

C. Wang

July 1993

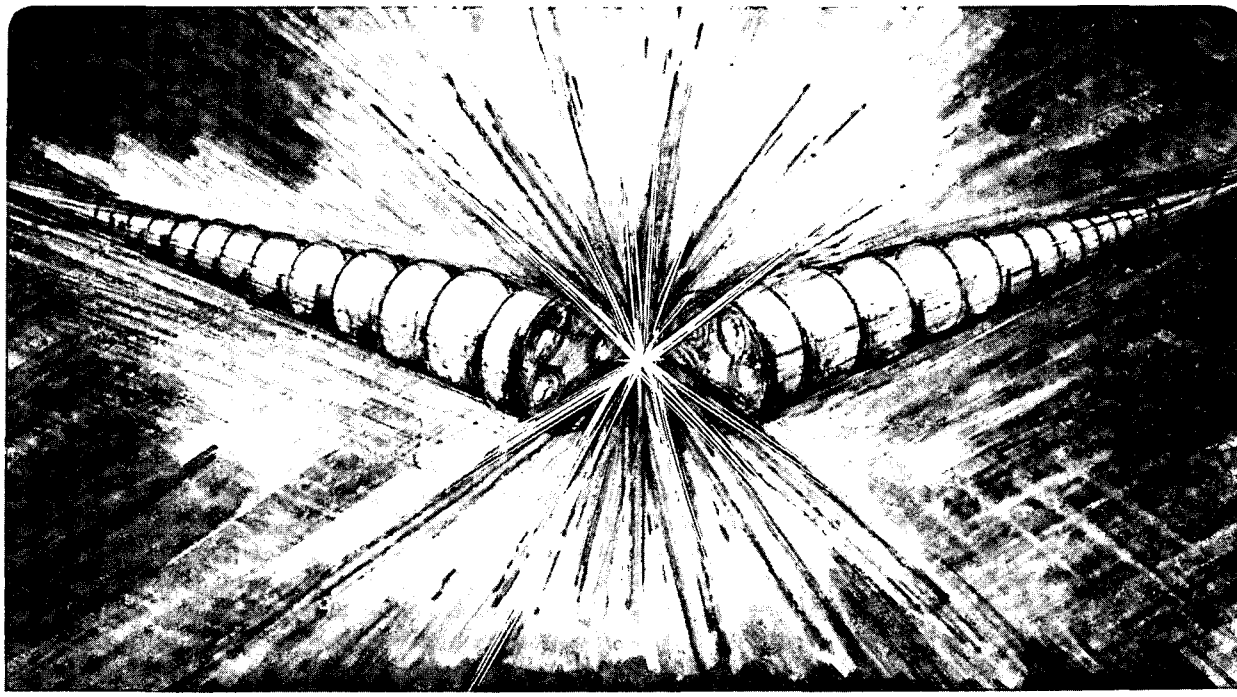

LOAN COPY
Circulates
for 4 weeks
Bldg. 50 Library.
LBL-33355
Copy 2

Prepared for the U.S. Department of Energy under Contract Number DE-AC03-76SF00098

DISCLAIMER

This document was prepared as an account of work sponsored by the United States Government. While this document is believed to contain correct information, neither the United States Government nor any agency thereof, nor the Regents of the University of California, nor any of their employees, makes any warranty, express or implied, or assumes any legal responsibility for the accuracy, completeness, or usefulness of any information, apparatus, product, or process disclosed, or represents that its use would not infringe privately owned rights. Reference herein to any specific commercial product, process, or service by its trade name, trademark, manufacturer, or otherwise, does not necessarily constitute or imply its endorsement, recommendation, or favoring by the United States Government or any agency thereof, or the Regents of the University of California. The views and opinions of authors expressed herein do not necessarily state or reflect those of the United States Government or any agency thereof or the Regents of the University of California.

LBL-33355

Monte Carlo Calculation of Multi-electron Effects on Synchrotron Radiation*

Chunxi Wang

Advanced Light Source
Accelerator and Fusion Research Division
Lawrence Berkeley Laboratory
University of California
Berkeley, CA 94720

July 1993

Paper Presented at the SPIE 1993 International Symposium on Optical Applied Science and Engineering
San Diego, CA
July 11-16, 1993

***This work was supported by the Director, Office of Energy Research, Office of Basic Energy Sciences, Materials Sciences Division of the U.S. Department of Energy, under Contract No. DE-AC03-76SF00098.**

Monte Carlo calculation of multi-electron effects on synchrotron radiation

Chunxi Wang

Lawrence Berkeley Laboratory, Advanced Light Source
1 Cyclotron Road, Mail Stop 2-400, Berkeley, CA 94720

ABSTRACT

The phase space distribution and time structure of an electron beam have fundamental influences on synchrotron radiation properties. These influences are due to the superposition of radiation from all electrons, each following a different trajectory. When the radiation wavelength is longer than the electron bunch length, coherent superposition occurs and results in the observed coherent synchrotron radiation. Usually the wavelength we use is much shorter, so incoherent superposition occurs and the emittance effect is the dominant multi-electron effect. The Monte Carlo simulation is a straightforward and generally valid approach to compute the multi-electron effects on synchrotron radiation. In this paper, we show how the Monte Carlo method can model these multi-electron effects systematically and discuss the statistical principles governing such simulation and their implication on the computing power requirement. We also describe the implementation of an efficient algorithm to calculate a single electron radiation spectrum, which is important to make the Monte Carlo simulation practical. Some calculated results are shown to demonstrate the methods. Comments on the usefulness and limitation of the Monte Carlo method are presented.

1. INTRODUCTION

Synchrotron Radiation (SR) is generated by billions of electrons, usually bunched, in an electron beam. The multi-electron effects dominate many features of the radiation. When the electrons radiate coherently, we observe coherent synchrotron radiation,[1] in which the radiation intensity is enhanced dramatically. Usually the electrons radiate incoherently and their effects, known as the beam emittance effects, tend to degrade the single electron radiation properties. In fact, the emittance effects are so important that a criteria for the third generation SR sources is based on the magnitude of electron beam emittance. Convolution of a single electron's radiation with electron phase space distribution is widely used to calculate the emittance effect. This method is based on the approximation that the radiation distributions of all electrons are related by a simple coordinate transformation. Another way to take into account all the multi-electron effects is the well-known Monte Carlo simulation method.[2]

The Monte Carlo method is a straightforward and generally valid approach to accommodate systematically the multi-electron effects in SR calculations. In fact, we can simulate an electron bunch, trace the trajectory of each electron and calculate its radiation, then superpose the radiation directly. However, such an approach is often too time consuming to be practical because of the large number of individual calculations of single electron radiation. Thus, a clear understanding of the statistical principles governing the multi-electron radiation process is important to an efficient simulation algorithm. Moreover, reduction of the computing time for each electron is extremely important to a practical Monte Carlo simulation. In this paper, we discuss the implementation of the Monte Carlo method, especially the statistical model governing the simulation of coherence effects. According to the statistical model, it is necessary to average the radiation intensity in addition to superpose electric fields of different electrons. It turns out that the intensity averaging process is the most time consuming requirement for the Monte Carlo simulations. Coherent synchrotron radiation and emittance effects are demonstrated. Following the discussion on the Monte Carlo method, we describe in detail the implementation of an efficient algorithm to calculate the single electron radiation. This algorithm, which is based on a recently reported concise expression of a classical radiation spectrum[3] and the fast Fourier transform (FFT) method,[4] can greatly reduce the computation required for the Monte-Carlo calculation. Algorithms discussed in this paper have been implemented in the program *RADID*.[5] Some results calculated for the ALS U5 undulator are presented to show the capabilities of *RADID* in handling the effects due to magnetic field errors, beam emittance, and finite observation distance. Finally, we make some comments on the Monte Carlo method based upon our experience.

2. MONTE CARLO SIMULATION OF MULTI-ELECTRON EFFECTS

2.1 Statistical model of the simulation

A basic physical quantity in radiation calculations is the flux (power) density spectrum I(ω):[6]

$$I(\omega) \propto \left| \int_{-\infty}^{\infty} E(t) e^{i\omega t} dt \right|^2 , \tag{1}$$

where **E**(t) is the electric field at the observation point. In principle, **E**(t) should be a linear superposition of the electric fields from all electrons. Suppose we have N electrons, thus:

$$E(t) = \sum_{j=1}^{N} E_j(t) . \tag{2}$$

The summation can be performed either before or after the Fourier transform based on the linearity of the transformation. Since the Fourier transform is a major time consuming calculation, it would be logical to perform the field amplitude superposition first if a large number of such superposition were all we need to simulate the multi-electron effects. In the following, we discuss the basic requirements in a simulation and evaluate the feasability of the above approach.

To simplify our discussion, let us consider the case that all $\mathbf{E}_j$ have the same form ε(t) but with different arrival time t_j, i.e.

$$E(t) = \sum_{j=1}^{N} \varepsilon(t + t_j) \tag{3}$$

According to the Fourier transform time shifting theorem, the spectrum becomes,

$$I(\omega) \propto \left| \int_{-\infty}^{\infty} \varepsilon(t)\, e^{i\omega t} dt \right|^2 \times \left| \sum_{j=1}^{N} e^{i\omega t_j} \right|^2 \tag{4}$$

$$= (\text{single electron spectrum}) \times \mathcal{N} ,$$

where the multi-electron effects are included in the factor $\mathcal{N}$ and we have,

$$\mathcal{N} \equiv |n|^2 \equiv \left| \sum_{j=1}^{N} e^{i\omega t_j} \right|^2 = N + \sum_{j \neq k} e^{i\omega(t_j - t_k)} . \tag{5}$$

Generally, t_j is a random variable. It is a common argument that, when t_j is distributed over a range larger than $2\pi/\omega$, the large number of terms in the summation of Eq. (5) will cancel each other and result in an incoherent superposition with the expectation value $\overline{\mathcal{N}} = N$; on the other hand, if $\omega t_j \ll 1$, coherent superposition occurs and $\overline{\mathcal{N}} = N^2$.

When the distribution of t_j is known, one can calculate the average value of $\mathcal{N}$ in detail. Let us assume that ωt_j has a Gaussian distribution with variance σ, it is easy to verify that:

$$\overline{\mathcal{N}} = N + N(N-1)\, e^{-\sigma^2} = \begin{cases} N^2 , & \sigma \to 0 \\ N , & \sigma \to \infty \end{cases} \tag{6}$$

So far, only standard procedures[7,1] have been used. Although the superposition of field amplitudes seems to account for the coherence effect, if one tries to implement the procedure, a subtle statistical problem is encountered. No matter how large N, $\mathcal{N}$ does not converge to the expected average value N of Eq. (6) in the incoherent limit.

To understand what the problem is, we calculate the variance of $\mathcal{N}$ in the above Gaussian distribution case and find,

$$\sigma_{\mathcal{N}}^2 = N(N-1) + 2N(N-1)(N-2)e^{-\sigma^2} - 2N(N-1)(2N-3)e^{-2\sigma^2} + 2N(N-1)(N-2)e^{-3\sigma^2} + N(N-1)e^{-4\sigma^2}$$

$$\to \begin{cases} 0 , & \sigma \to 0 \\ N^2 - N , & \sigma \to \infty \end{cases} \tag{7}$$

We see that the fluctuation $\sigma_{\mathcal{N}}$ is nearly equal to the expectation value N. In fact, this result is quite independent of the detailed distribution of the random variable t_j. Here, we give the general statistical properties of n and $\mathcal{N}$ without proof.[8,9]

- For a series of independent random variables t_j the quantity $n=\sum_{j=1}^{N} e^{i\omega t_j}$ is a random variable; in the case of $N\rightarrow\infty$, $\mathrm{Re}\{n\}$ and $\mathrm{Im}\{n\}$ are independent random variables that follow the Gaussian distribution law.
- In the above Gaussian limit, $\mathcal{N}\equiv|n|^2$ is a random variable, whose probability distribution is the negative exponential law:

$$P_{\mathcal{N}}(x)=\frac{1}{\overline{\mathcal{N}}}e^{-x/\overline{\mathcal{N}}} \tag{8}$$

with expectation $\overline{\mathcal{N}}=N$ and variance $\sigma_{\mathcal{N}}=N$.

The statement on n can be understood intuitively through the well known central limit theorem though a rigorous proof is rather involved. The statement on $\mathcal{N}$ can be derived from the properties of n.

The reason we do not observe such fluctuations in experiments (In fact, similar fluctuations do exist in the laser speckle phenomena) can be explained by the intensity average over a long observation interval or a finite bandwidth, etc. Detailed explanation involves fundamental measurement theories.[9,10]

For our modeling purpose, let us simply consider a summation over M similar experiments. The observed quantity now is $\Pi=\sum_M I_i$, which is a random variable resulting from the summation of M independent random variables that have the same negative exponential distribution. From standard probability theory we know that, Π follows a Chi-square distribution,[8,10]

$$P_{\Pi}(x)=\frac{1}{\overline{\mathcal{N}}^M}\frac{1}{\Gamma(M)}x^{M-1}e^{-x/\overline{\mathcal{N}}} \tag{9}$$

with expectation $\overline{\Pi}=MN$ and variance $\sigma_{\Pi}=\sqrt{M}\,N$. We see that the signal to noise ratio is $\sqrt{M}$ after the intensity averaging.

From the above discussion we see that, in order to simulate the multi-electron effects resulting from superposition of the radiation fields of N electrons, two averaging steps are involved. One is the summation of the electric fields of N electrons, the other is the summation of M independent intensity observations. So the total electrons needed in a simulation is NM. Because the computation required for such simulation is proportional to NM, a reasonable choice of N and M is very important. As we know that $1/\sqrt{M}$ determines the calculation accuracy, it should be on the order of 1000. This is a very strong requirement that limits the efficiency of the Monte Carlo simulation method. One may think that N should also be a large number according to the argument following Eq. (5). Fortunately, this is not the case. From the above discussion we see that N may need to be large enough to guarantee that the random variable n approaches the limit determined by the central limit theorem. Nonetheless, $N=4$ usually gives a good approximation.[8] This means that it does not help much in reducing the computation by performing the electric field superposition in the time domain. Although our discussion is based on a special case Eq. (3) instead of Eq. (2), it is clear that the two step averaging procedure is appropriate for the general simulation of multi-electron effects. The intensity averaging process is indispensable and turns out to be the main factor that limits the efficiency of the Monte Carlo method. The general signal to noise ratio is proportional to (though not exactly equal to) $1/\sqrt{M}$, which provides a rough estimate of the amount of computation required and the simulation accuracy.

2.2 Implementation of the Monte Carlo method

Following the above model, the implementation of the Monte Carlo method is quite straight forward. In fact, the simplicity in implementation and the general applicability of the method are an attractive aspect of the Monte Carlo method. We simulate an electron bunch with a large number of samples, which are generated randomly according to the beam transverse and longitudinal phase space distributions. For each sample, we use its position and velocity as the initial conditions, trace its trajectory through the magnetic field of a device and then calculate its radiation field $\mathbf{E}_j$. Such a routine is repeated for the NM electron samples. The electric fields of every successive N samples are superposed and then their radiation intensity is calculated. Finally, the M intensity values are summed and averaged by the number of samples. In the following, we discuss some details concerning each process.

In a storage ring, the transverse phase space distributions of an electron beam are given by:

$$P(x,x')=\frac{1}{2\pi\varepsilon_x}e^{-\frac{1}{2\varepsilon_x}\left(\gamma_x x^2+2\alpha_x x x'+\beta_x x'^2\right)}dx\,dx', \tag{10}$$

where

$$\langle x^2 \rangle = \beta_x \varepsilon_x; \ \langle x'^2 \rangle = \gamma_x \varepsilon_x; \ \gamma_x = (1+\alpha_x^2)/\beta.$$

ε_x is the beam emittance, β_x is the amplitude function and γ_x, α_x, are the Twiss parameters; the subscript x represents either horizontal or vertical direction. Transforming to a standard binary normal distribution, we have:

$$P(x,x') = \frac{1}{2\pi\sigma_x\sigma_{x'}\sqrt{1-\rho^2}} e^{-\frac{1}{2(1-\rho^2)}\left(\frac{x^2}{\sigma_x^2} - 2\rho\frac{xx'}{\sigma_x\sigma_{x'}} + \frac{x'^2}{\sigma_{x'}^2}\right)} dx\, dx', \tag{11}$$

where

$$\sigma_x = \sqrt{\beta_x \varepsilon_x}; \quad \sigma_{x'} = \sqrt{\gamma_x \varepsilon_x}; \quad \rho = \sqrt{1-(\varepsilon_x / \sigma_x\sigma_{x'})^2}.$$

This form of random distribution can be simulated by standard library routines using the transformation:[2]

$$\begin{aligned} x &= x_0 + \sigma_x\sqrt{-2\ln u}\left(\sqrt{1-\rho^2}\cos 2\pi\upsilon + \rho\sin 2\pi\upsilon\right), \\ x' &= x_0' + \sigma_{x'}\sqrt{-2\ln u}\ \sin 2\pi\upsilon, \end{aligned} \tag{12}$$

where u and υ are random variables uniformly distributed in the interval (0,1).

The longitudinal or time structure of a bunch is simulated independently by using a Gaussian distribution with an rms bunch length σ_z. Of course, there are many other possible bunch structures in a linac. In fact, we can accommodate as much information as necessary (e.g. beam energy spread) for the electron beam simulation.

A major task in the simulation is to trace each electron trajectory in the magnetic device. In principle, the trajectories can be calculated numerically. However, such a process is usually rather time consuming because thousands of iterations are required. A useful approximation is to relate all electron trajectories to a reference central orbit through a simple linear transformation:

$$\begin{aligned} x(z) &\approx \beta_{0x}(z-z_0) + X(z) \\ y(z) &\approx \beta_{0y}(z-z_0) + Y(z) \\ Dp(z) \equiv ct - z &\approx Dp0(z) + \tfrac{1}{2}(\beta_{0x}^2 + \beta_{0y}^2)(z-z_0) + [\beta_{0x}X(z) + \beta_{0y}Y(z)] \end{aligned} \tag{13}$$

where X(z), Y(z) and Dp0(z) specify the central orbit. Such an approximation is basic to the convolution method of calculating the emittance effect. However, in the Monte Carlo simulation method, it is just a useful approximation to save computation. The central orbit can be calculated in many ways and a measured magnetic field can be used also, which is important in order to take into account the field error effects.

The main task of calculating the radiation field of each electron is necessary though rather time consuming. The transformation trick similar to that used in the trajectory calculation usually does not help because of the vast amount of information (both spatial and energy domain) involved in the radiation spectra. Here, we are talking about a general spectrum that has no analytical expression. A complete discussion of the single electron radiation calculations is a topic beyond this paper. However, because of its importance to a practical simulation, we describe in detail the implementation of an efficient algorithm to calculate a single electron spectrum in section 3.

2.3 Simulation of coherent synchrotron radiation

Coherent synchrotron radiation was observed in an experiment using the Tohoku 300 MeV electron linac in 1989 for the first time. It supports the simple theory that: when the radiation wavelength is longer than the electron bunch, all electrons in the bunch radiate coherently like a single particle. This phenomena is well accommodated in the statistical model presented in section 2.1. Here we show some simulation results to demonstrate our discussion about the statistics.

In these simulations, we use parameters similar to the experiment in Ref. 1. The electron beam energy E_e=150 MeV and the bending radius R=2.44 m. The electron bunch length σ_z=0.25 mm and beam emittance is zero. In Fig. 1, we show the influence of different M on the simulation with constant N=10. The coherent and incoherent superposition results appear naturally in the same simulation routine. The coherence occurs in the wavelength range that is longer than the bunch length. The maximum coherence enhancement is exactly 10, the number of electrons involved in the electric field superposition. The fluctuations discussed in section 2.1 also appear and go down with the increase of M. We also see that the fluctuations occur only in the incoherent regime. This is because the linear superposition process converges to the average value in the coherent regime; see Eq. (6).

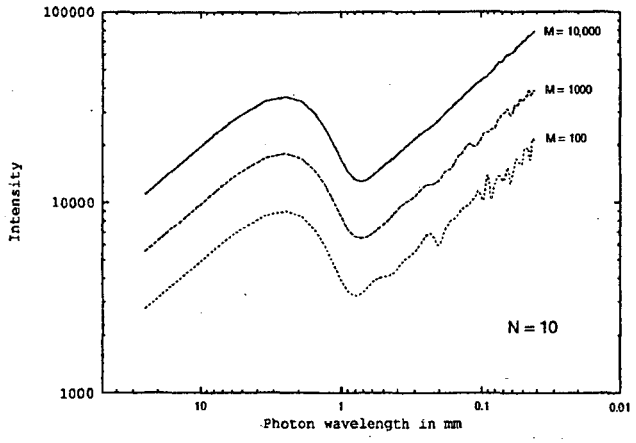

Fig. 1. The intensity averaging process. Three curves use the same N=10 but different M values as labeled. They are shifted vertically to show the fluctuations clearly.

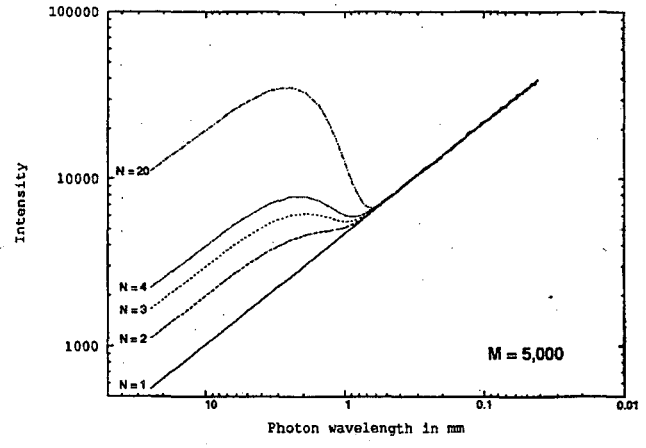

Fig. 2. Linear enhancement of intensity with the increase of N in the coherence regime. Influence of N on the statistical fluctuations is barely noticeable.

In Fig. 2, we show the increase of coherence enhancement with N while M=5000. As expected, the intensity goes up quadratically (linearly relative to the incoherent values) with N in the coherence regime. The influence of N on statistical fluctuations is barely noticeable. We also see that the N=1 case, in which no electric field superposition process is involved, gives the incoherent result. This allow us to neglect completely the field superposition process and makes the simulations of other multi-electron effects more efficient when we are interested in the incoherent regime.

Though the above procedure works well to simulate the coherence effect between electrons, it seems impractical to simulate the millions of electrons in a real bunch. However, we can use this procedure to extract the electron bunch form factor[1] by using the result obtained with a small number of N. The problem with this method is that we may lose some information around the region that the coherence enhancement just begins to build up. With small N, such enhancement may be lower than the simulation fluctuation errors. There is a tradeoff between accuracy and efficiency.

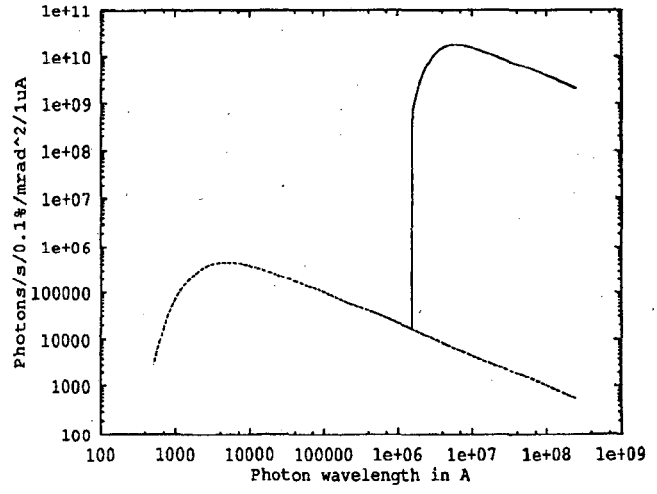

Fig.3 Simulation of a coherent SR experiment.

In Fig. 3 we show a result simulated in this way. As above, we use the same reported case. The parameters used are N=10, M=1000. If the coherent enhancement is less than 10%, it is disregarded and considered to be noise. The number of electrons in a bunch in this case is 3.6×10^6 and σ_z=0.054mm (corresponding to the reported 0.25mm full length half maximum bunch length). The average beam current is 1μA. The solid curve is the simulation result. The dashed curve is the single electron spectrum. All of the main features are comparable with experiment. One can also see the cutoff at the edge. Here our purpose is to show the Monte Carlo method rather than explain the experiments, so some factors such as acceptance angle, beam size, and energy spread have not been taken into account.

Although it may not be necessary to use the relatively inefficient simulation method to calculate the coherence enhancement of bending magnet SR, the method described in this paper has the potential to simulate much more

complicated experiments in which coherent superposition of radiation from different electrons is important whereas analytical analysis may be too involved.

2.4 Simulation of emittance effects

Unlike the above coherence effect between electrons, the emittance effects are much more familiar in most SR applications and it is of practical importance to be able to calculate these effects accurately. Through a very simple mechanism--incoherent superposition of the radiation from different electrons, the electron beam emittance can affect most aspects of the radiation properties of all kinds of devices. The general applicability of the Monte Carlo simulation, as described in section 2.2, makes it an appealing method to calculate emittance effects. Since our purpose here is to examine the Monte Carlo method rather than electron beam emittance effects in general, we just show a few simulations of an interesting case: the transition of a high K undulator spectrum to a wiggler spectrum, in which the beam emittance plays an important role.

The periodic field structure in an undulator or wiggler makes its radiation spectrum consist of discrete harmonics, which results from the coherent interference of the radiation from different parts of a single electron trajectory. However, we usually observe the harmonic spectrum in a low K undulator and a broad bending magnet like spectrum in a high K wiggler. This is because the relative spacing between the harmonics decreases as K^{-3} (K>>1) at the critical energy, around which most power is radiated[11,12]. So for a large enough K, the harmonics become so close that they are smoothed by the beam emittance or finite observation resolutions. In Figs. 4-7, we show transition from an undulator to a wiggler through the on-axis flux density spectra of a 14 period sinusoidal device with λ_u=20cm, K=10 and E_e=1.5 GeV.

Fig. 4 shows the single electron spectrum calculated with the algorithm described in the next section. There are hundreds of equally spaced undulator harmonics with a bending magnet spectrum-like envelope (a few glitch-like spikes at high energy have been removed). Only odd harmonics are present. The blowup shows the well-defined harmonics in detail at high energy. The following three graphs show the on-axis spectrum including emittance effects with ε_x=620nmrad, σ_x=2.6mm, $\sigma_{x'}$=0.58mrad and ε_y=48nmrad, σ_y=0.47mm, $\sigma_{y'}$=0.17mrad.

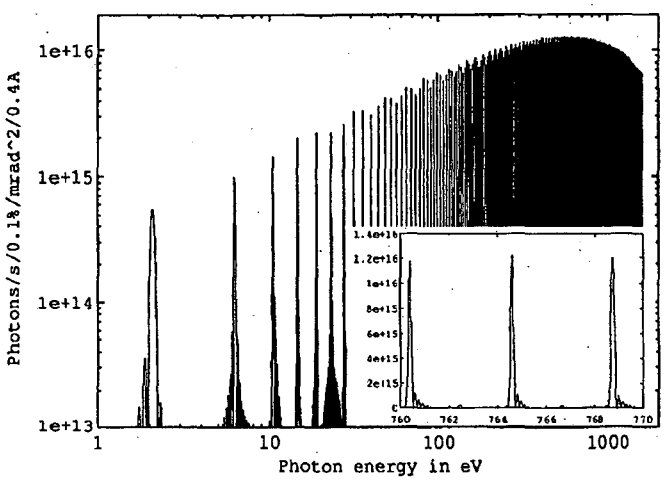

Fig. 4. On-axis flux density spectrum of a single electron. See details in blowup.

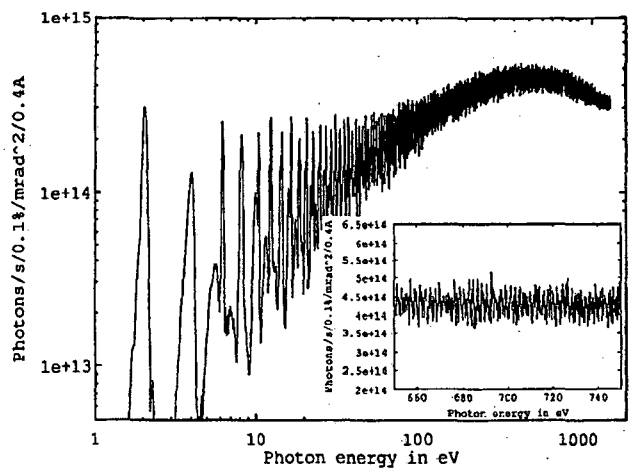

Fig. 5. Emittance included spectrum calculated with 3600 electron samples.

Fig. 5 shows the spectrum of Fig. 4 including the emittance effects. At low energy, as in a typical undulator, the harmonics are broadened and even harmonics appear also. The peak reduction due to the emittance can roughly be accounted for by $1/\sqrt{(1+(\sigma_{x'}/\sigma_{r'})^2)(1+(\sigma_{y'}/\sigma_{r'})^2)}$, where $\sigma_{r'}$ is the angular width of a harmonic. As the energy increases, the harmonics merge into a broad bending magnet like spectrum. The peak reduction at high energy is roughly $1/\sqrt{1+(\sigma_{y'}/\sigma_{r'})^2}/N$, but here $\sigma_{r'}$ is the bending magnet vertical angular distribution width. The factor 1/N means that the coherence enhancement among the radiation of different parts of the trajectory is killed by the beam emittance. So this device behaves like an undulator at low energy and like a wiggler at high energy. The fluctuations are still quite noticeable even with 3600 electron samples in this case.

In order to examine the electron ensemble size influence, we calculate the same spectrum with a much smaller M=400 and show the result in Fig. 7. The first few harmonics are plotted in Fig. 6. The two curves correspond to different M, 3600 vs. 400. We see that, in the undulator regime, the much smaller ensemble size gives nearly the same result, especially at the odd harmonics. This is very important to practical applications of the Monte Carlo method. Comparing Fig. 7 and Fig. 5, especially the blowups, we see that the fluctuation decreases as $1/\sqrt{M}$, which is the expected result. In the wiggler regime, it is possible to extract a much more accurate spectrum from the fluctuations by a least squares fit or other methods. From Figs. 5 and 7 we see that the transition starts around 50 eV, which is about $0.5\lambda_u\sigma_x^2$ in wavelength and independent of the deflection parameter K and the harmonic number n. This gives an upper photon energy limit for a certain storage ring, above which no undulator harmonics can be generated.

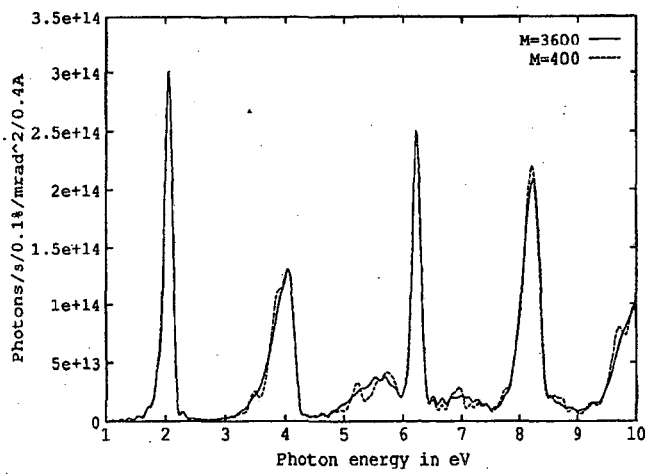

Fig. 6. The first few harmonics of the emittance included spectra calculated with a different ensemble size.

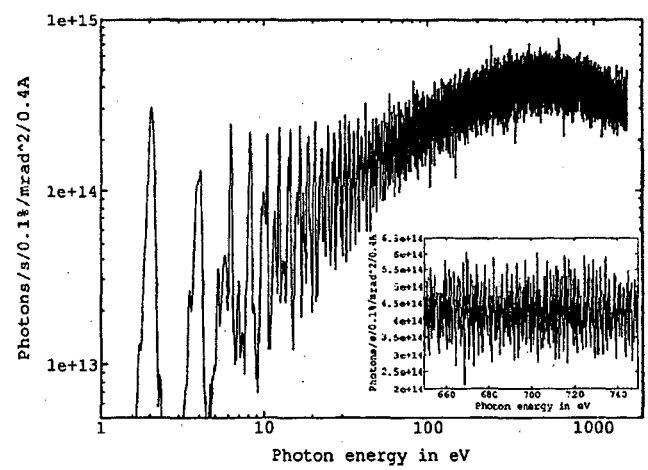

Fig. 7. Same as Fig. 5 but using a much smaller M=400. So the fluctuations is 3 times larger.

3. AN EFFICIENT ALGORITHM TO CALCULATE A SINGLE ELECTRON SPECTRUM

3.1 Theoretical and computational background

The primary goal of most radiation calculations is to obtain the energy spectrum. As discussed above, an efficient method to calculate a single electron spectrum is very important to the Monte Carlo simulation. It is well known that the spectrum, which is the energy radiated by an electron into a unit frequency interval and unit area, is given by:[6]

$$\frac{d^2I}{d\omega dA}=\frac{1}{4\pi\varepsilon_0}\frac{e^2}{4\pi^2c}\left|\int_{-\infty}^{\infty}\left\{\frac{\mathbf{n}\times[(\mathbf{n}-\beta)\times\dot{\beta}]}{(1-\mathbf{n}\cdot\beta)^2R}+\frac{(\mathbf{n}-\beta)c}{\gamma^2(1-\mathbf{n}\cdot\beta)^2R^2}\right\}e^{i\omega(\tau+\frac{R(\tau)}{c})}d\tau\right|^2. \tag{14}$$

The far field approximation form is:

$$\frac{d^2I}{d\omega d\Omega}=\frac{1}{4\pi\varepsilon_0}\frac{e^2\omega^2}{4\pi^2c}\left|\int_{-\infty}^{\infty}\mathbf{n}\times(\mathbf{n}\times\beta)e^{i\omega\left(\tau-\frac{\mathbf{n}\cdot\mathbf{x_e}}{c}\right)}d\tau\right|^2. \tag{15}$$

Despite a few analytical results for some ideal cases, such as the bending magnet or the sinusoidal undulator radiation spectra, it is often necessary to calculate Eq. (14) numerically. In order to take into account the magnetic field errors, finite observation distance, etc., an algorithm capable of computing the spectrum of an arbitrarily moving electron is required. Usually such calculations are rather complicated and time consuming.

The main difficulty of numerical calculation of Eq. (14) comes from the fast oscillating phase term which makes ordinary integration routines very inefficient or even unworkable. A natural idea is to use the FFT method because a spectrum is basically determined by a Fourier transform of the electric field, and the FFT method is a well known efficient numerical algorithm to perform such a transformation. However, Eq. (14) is developed mainly for analytical calculations and is rather awkward for numerical computation. In search of a better way to calculate a spectrum, a much more concise expression of a single electron radiation spectrum was found:[3]

$$\frac{d^2I}{d\omega dA}=\frac{\alpha\hbar\omega^4}{4\pi^2c^2}\left|\int_{-\infty}^{\infty}\mathbf{n}(ret)e^{i\omega t}dt\right|^2. \tag{16}$$

The expression in Eq. (16) is generally equivalent to Eq. (14) and provides a much more efficient way to calculate the spectrum.

As discussed in Ref. 3, Eq. (16) has several advantages for numerical radiation calculations. First, it is equivalent to Eq. (14) under the condition $R \gg \gamma\lambda$, where γ is the relativity factor and λ is the radiation wavelength. It is clear that this condition is satisfied in most practical SR applications even in the region where the near field effect[13] is significant. So Eq.(16) can be used for all situations in SR calculations. Secondly, it is in an exact form of the Fourier transform and we can take advantage of the FFT method directly. Usually we can get the entire spectrum with the FFT method in the time to calculate one frequency point by ordinary integration routines. Thirdly, the function to be transformed is much easier to calculate, which is important for an efficient algorithm. Moreover, to calculate **n**, only trajectory information is required. This may be important when the amount of required computer memory is of concern. Considering all the advantages of Eq.(16), we believe that it provides the most efficient algorithm to perform SR spectrum calculations when the FFT is applicable. In the following section, we discuss several important issues in the implementation of this algorithm. Some results calculated with this algorithm are shown in section 4.

3.2 Implementation of the algorithm

To use Eq. (16) numerically, we first change the integration limits because they are impractical for numerical calculations. A natural choice is the physical boundaries of a device. Unlike Eq.(14), the integrand **n**(t) usually does not vanish outside a magnetic field. So we have to include two boundary terms and Eq. (16) can be changed to:

$$\frac{d^2I}{d\omega dA} = \frac{\alpha\hbar}{4\pi^2}\left|\frac{\mathbf{n}\times(\mathbf{n}\times\beta)}{(1-\mathbf{n}\cdot\beta)R}e^{i\omega t}\Big|_{t_a}^{t_b} - i\frac{\omega}{c}\mathbf{n}e^{i\omega t}\Big|_{t_a}^{t_b} - \frac{\omega^2}{c}\int_{t_a}^{t_b}\mathbf{n}e^{i\omega t}dt\right|^2 \tag{17}$$

For a detailed discussion of the boundary terms, please refer to Ref. 14. The integration term in Eq. (17) is suitable for numerical calculation while the boundary terms are easy to take care of.

In order to use the FFT method to calculate the integration of Eq. (17), we must sample the function $\mathbf{n}(t)$ at equally spaced discrete points in the time domain. To do this, we first calculate the direction vector **n**. Noticing that **n** should be calculated in the electron time frame and the Fourier transform is done in the observer time frame, we have to change the time frame first. Usually, the trajectory is calculated with the longitudinal coordinate z of a magnetic device as the independent variable. Both the trajectory and $t(z)$ are calculated at a constant increment of z and this information is stored in arrays. Then we interpolate these data to obtain $\mathbf{n}(t)$ at the sampling points. The sampling interval Δt is chosen to satisfy the Nyquist criteria.[4]

There is another issue before we do the FFT. Generally, $\mathbf{n}(t)$ is not equal to zero at the boundary points t_a and t_b. This turns out to cause a serious problem for the FFT method. To solve this problem, we introduce a new quantity $\tilde{\mathbf{n}}$ by subtracting a linear vector term from **n**:

$$\tilde{\mathbf{n}}(t) = \mathbf{n}(t) - \mathbf{n}(t_a) - \frac{\mathbf{n}(t_b)-\mathbf{n}(t_a)}{t_b - t_a}(t - t_a) \tag{18}$$

The new function $\tilde{\mathbf{n}}(t)$ is suitable for FFT while the linear term can be integrated analytically and combined with the boundary terms.

The computing accuracy of both $\tilde{\mathbf{n}}$ and t is very important but not easy to maintain, because the leading term of $\tilde{\mathbf{n}}$ is a constant and the absolute error of ωt has to be much smaller than one while its magnitude may change several orders. Fortunately, the accuracy still can be maintained even with single precision variables through careful programming. There are several other typical issues about the usage of FFT routines to make the calculation more efficient. For example, usually only the two transverse components, Ex and Ey, need to be calculated. So we combine the two real quantities into a complex one and perform the FFT only once to get all the information required.

3.3 Limitation of the algorithm and other approaches

Although the above algorithm is quite versatile, it has limitations and disadvantages which are due to the Fourier transform method. The main limitation comes from the Nyquist criteria. To avoid aliasing, there should be at least 2 sampling points in each period at the highest frequency. Usually, the radiation spectrum is not band-limited and we have to choose a cutoff frequency. Let us consider a typical case, an N period undulator with deflection parameter K. The critical harmonic number N_c is given by:[11]

$$N_C = \frac{3}{4}K\left(1+\frac{K^2}{2}\right) \sim \frac{3}{8}K^3 \quad , \quad \text{for } K \text{ large} \tag{19}$$

Suppose we choose $10N_C$ as the cutoff frequency, the number of sampling points N_S should be $20NN_C \sim 7.5NK^3$, which goes up very fast with K. For example, if N=100 and K=10, the required sampling points is on the order of 2^{20} or 10^6, which may cause difficulties for limited computer memory resources. The calculation speed is approximately proportional to $N_S \log_2 N_S$, so the calculation will be slowed down very quickly also as K increases. This means that methods based on the FFT are not suitable for wiggler type, high-K devices.

To overcome this difficulty, the FFT-Filon method[8] may be a useful algorithm. Another option is to follow a completely different idea. In general, for high K devices, the phase term in Eq. (14) is oscillating so fast that the stationary phase method[5] gives a good approximation. This idea has been developed into another efficient algorithm for high K devices with arbitrary beam trajectory.

4. SOME APPLICATIONS AND COMMENTS ON THE MONTE CARLO METHOD

4.1 RADID: software for synchrotron radiation calculation

RADID is software developed by the author for general SR radiation calculations including all relevant factors, such as magnetic field errors, beam emittance, and near field effects. The radiation properties that can be calculated include all the information available in the Stokes description[7] of a radiation field. All kinds of 2D or 3D insertion devices can be calculated. Measured magnetic fields can be used in order to take into account the field error effects. Various flux or power distributions in the photon energy and/or angular space can be obtained. The described Monte Carlo simulation method and the single electron radiation calculation algorithm have been integrated into *RADID*. So all kinds of multi-electron effects, especially the emittance effects, can be evaluated. Absorption of windows, filters, and so on, can be included by using a database of the atomic scattering factors of all elements. Despite versatility, efficiency of the software is of concern also. Special efforts have been put into the development of efficient algorithms. The algorithm discussed in section 3 forms the basis of the undulator radiation calculation method employed in *RADID*. An algorithm, based on the stationary phase method, is used to calculate wiggler type radiation. In the following we show some results of the application of *RADID* on the ALS U5 undulator spectrum.

4.2 Beam emittance, field error, and near field effects on the ALS U5 undulator spectra

To show the usefulness of the Monte Carlo simulation method and the single electron spectrum calculation algorithm addressed above, we present some applications for a real device, the ALS IDA, which has 89 periods of 5 cm each. Again, our main purpose here is to examine the calculation methods; only a few interesting cases are presented. Due to the length of the U5, many practical factors become significant to the radiation spectra. So the radiation calculations become a real challenge. As shown in the following, the method presented in this paper works well.

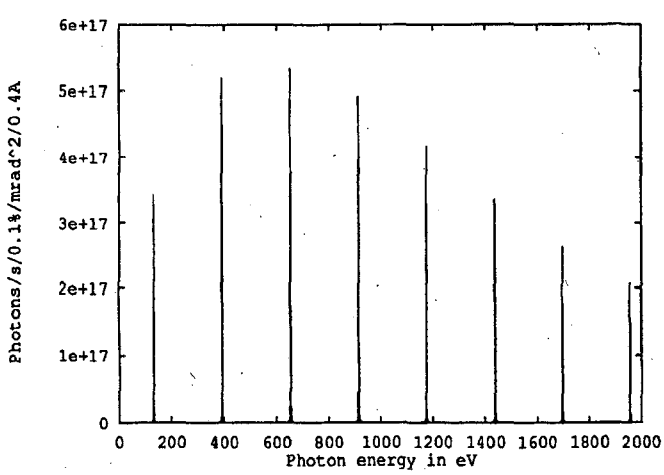

Fig. 8. On-axis spectrum of the ideal field.

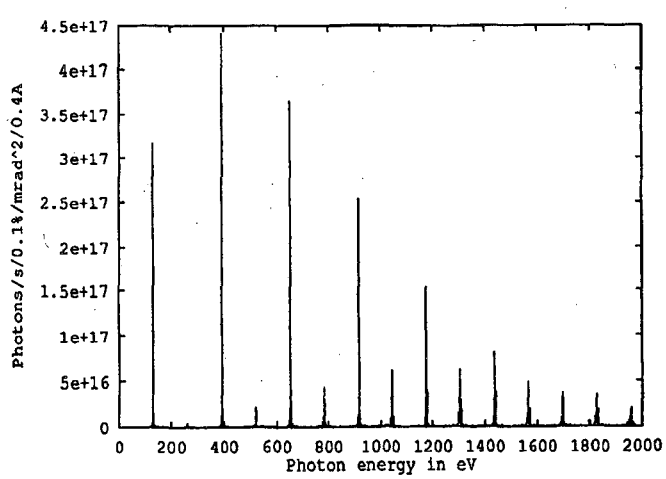

Fig. 9. On-axis spectrum of the measured magnetic field.

The physics of the effects shown below is well known, so only a brief description of each graph is included. In all the following calculations, we choose a medium magnetic gap 23mm, at which a precisely measured magnetic field is available.[15] The deflection parameter $K_{eff} = 2.13$. In Figs. 8-11, we show the on-axis spectra at an observation distance 100m. These graphs clearly show the magnetic field error and emittance effects on the spectrum.

Fig. 8 shows the on-axis spectrum calculated using the ideal effective field which consists of a sinusoidal field and one half peak pole at each end. The peak field value is $B_{eff} = \sqrt{B_1^2 + B_3^2/9 + B_5^2/25 + \cdots}$, where the B_1, B_3, B_5 etc. are the harmonics in the measured field. We see rich harmonics in the spectrum due to a relatively large deflection parameter. Fig. 9 shows the same spectrum but using the measured magnetic field. The spectrum is calculated at 18.8 μrad off-axis because of the trajectory drift due to random field errors and a dipole kick at the end. Compared to Fig. 8, the field error effect is significant at high harmonics.

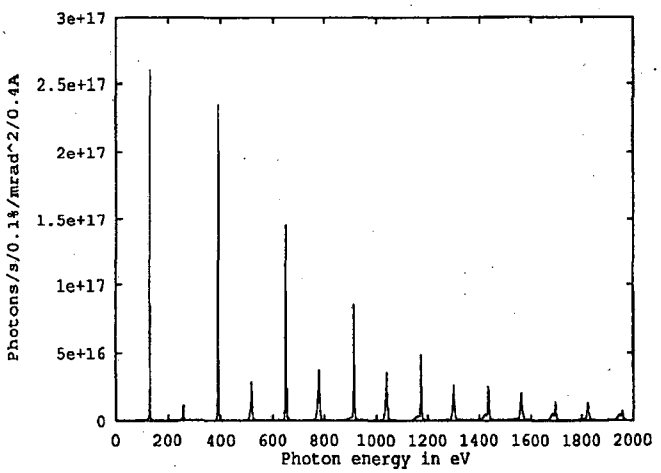

Fig. 10. On-axis spectrum of the measured field with ALS emittance included.

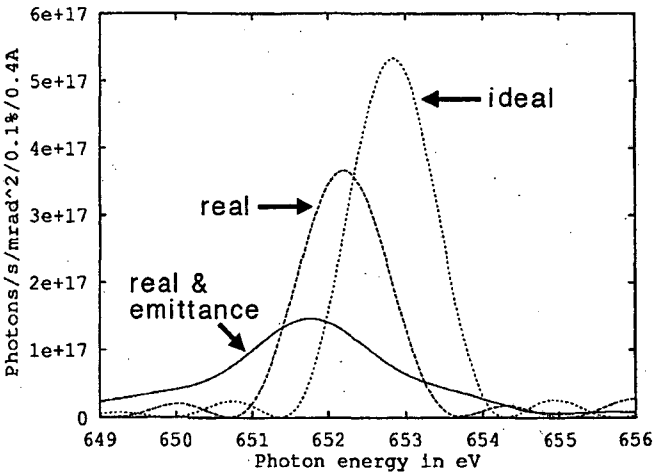

Fig. 11. On-axis spectra at the 5th harmonic, shows the field error and emittance effects in detail.

Fig. 10 shows the same case but with ALS emittance included. We see that the emittance effect is very large. Both the field errors and the beam emittance tend to kill the higher harmonics. Fig. 11 compares the Figs. 8-10 at the 5th harmonic in detail. Up to the 5th harmonic, the flux density reductions satisfy the specification requirement for the device. A much more complete evaluation of the field error effect on the spectral quality of U5.0 is presented in Ref. 16.

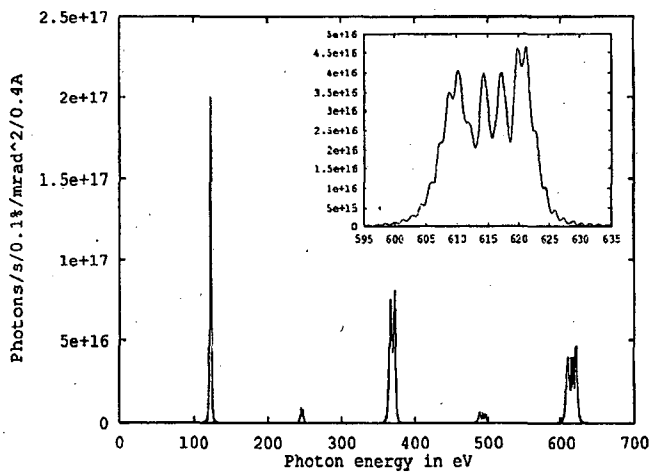

Fig. 12. Spectrum at 0.15mrad off-axis, no emittance.

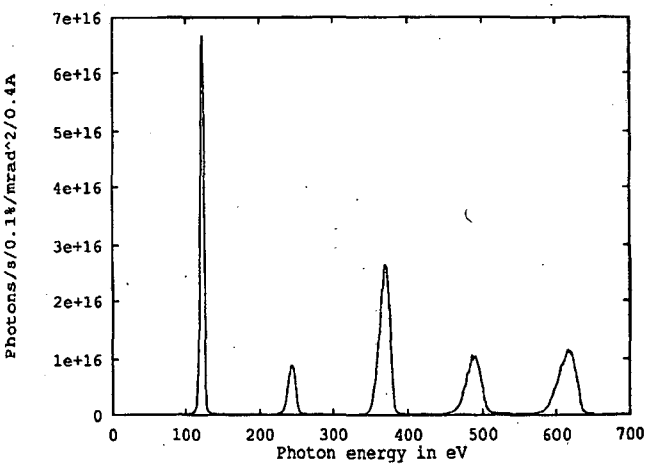

Fig. 13. Spectrum at 0.15mrad off-axis, ALS emittance.

In the next two graphs, we show the spectra calculated at 0.15mrad off-axis and an observation distance D=16m. According to R.P. Walker,[13] there should be significant near field effects. The Walker's parameter $W=L^2\theta^2/2\lambda D=7$ at the 5th harmonic in this case, while $W_{max}=nL^2/\lambda_u D=124$. As claimed in section 3.1, the algorithm is capable of handling the near field effects, which is demonstrated in Figs. 12-13.

Fig. 12 shows the near field effect without emittance. This result is comparable to Walker's result. The inserted graph shows the 5th harmonic in detail. Fig. 13 is the same as Fig. 12 but with ALS emittance included. We see that the fine peak structure due to near field effect is smoothed in this case. Both the near field and emittance effects are rather significant. Results presented here confirm that our method can accommodate all these effects.

4.3 Comments on the Monte Carlo method

As shown above, the Monte Carlo simulation method is capable of taking into account the multi-electron effects in SR spectrum calculations. Combining it with the single electron radiation calculation algorithms, we obtain a rather versatile method to compute the radiation properties. However, the efficiency of the Monte Carlo method is still a problem. As discussed in section 1, the typical CPU time needed for a Monte Carlo simulation is several thousands of similar runs of a single electron. Depending on the device parameters used, the single electron spectrum calculation takes from a few seconds to a few minutes on a SUN IPX workstation. So a simulation for a long device like U5, usually takes a few hours to obtain an entire emittance-included spectrum at one observation point for a large K value. Most difficult is calculations of emittance included angular (integrated) spectra. Usually, the angular integration process is as time consuming as the Monte Carlo simulation. So in some cases, other methods based on ideal analytical single electron spectra and various approximations may be more suitable. A representative program in this class is URGENT[17]. However, many factors like the field error effects can not be taken into account in this way. A promising approach to obtain an angular integrated spectrum is to introduce a suitable phase space distribution of electrons in the Monte Carlo simulation method. The efficiency of such a Monte Carlo integration is similar to the simulation of multi-electron effects. However, the angular integration and the simulation of emittance effects are naturally combined in the same routine; so there is no extra cost.

In addition to the Monte Carlo simulation, another well known method to perform the emittance average is the convolution of a single electron spectrum with the electron phase space distribution as shown in Eq. (20).[11]

$$\frac{d^2I}{d^2\varphi}(\varphi)=\int\frac{d^2I^0}{d^2\varphi}(\varphi-\varphi_e)\ g(\varphi_e)d^2\varphi_e \tag{20}$$

Here I^0 is the single electron spectrum and g is the angular distribution of the electron beam. Strictly speaking, the convolution method is not as generally valid as the Monte Carlo method; but in practical applications, both methods can be used to compute the emittance effect and a numerically calculated single electron spectrum can be used. So an important issue is which method is more efficient. To perform the convolution for one observation point, the two dimensional angular distribution is required. So a large number of single electron spectra at different angular positions have to be calculated. This makes the convolution method as time consuming as the Monte Carlo method to obtain an emittance included spectrum at one photon energy and observation point. For a few photon energies, the convolution method is perhaps somewhat more efficient. But for an entire spectrum, the convolution method is much slower because the convolution process has to be done for each photon energy; moreover, the 3D spectrum information has to be stored or recalculated, which is very difficult in either case. So, whenever the single electron spectrum has to be calculated numerically, the Monte Carlo simulation is a very competitive method to calculate the emittance effects.

The simulation calculation discussed in this paper neglects all interactions between electrons, which is valid for SR. It is possible to extend the Monte Carlo method to accommodate the interactions (e.g. in the trajectory calculation routine) and simulate the self-amplified spontaneous emission process. However, this most likely requires a super-computer.

5. CONCLUSION

In this paper, we described the Monte Carlo simulation method used in our SR calculations. The two step averaging procedure (amplitude superposition and intensity averaging) works well to simulate the multi-electron effects. A statistical model of our simulation is discussed and the computing power requirement is estimated. Different aspects of the multi-electron effects on synchrotron radiation can be accommodated systematically in our simulations, especially the coherence processes between electrons or different parts of the trajectory of a single electron. The transition from coherent SR to incoherent SR and from coherent undulator radiation to incoherent wiggler radiation are simulated. We also described the implementation of a very efficient algorithm to calculate the general single electron radiation spectrum. This algorithm makes it practical to calculate a radiation spectrum by the Monte Carlo simulation on workstation level computers. All

these algorithms have been integrated into the program *RADID*, which aims at a generally applicable and efficient numerical tool to calculate the SR properties. Some results calculated for the ALS U5 undulator demonstrate the power of *RADID*.

6. ACKNOWLEDGMENTS

The author would like to acknowledge some helpful discussions with K. J. Kim and B. M. Kincaid. Special thanks are due to K. Halbach for his suggestion leading to Eq.(18). I also would like to thank my colleagues R. Schlueter and S. Marks for their proofreading of the manuscript.

This work was supported by the Director, Office of Energy Research, Office of Basic Energy Science, Materials Science Division of the U.S. Department of Energy, under contract No. DE-AC03-76SF00098.

7. REFERENCES

1. K. Ishi, et al., "Spectrum of coherent synchrotron radiation in the far-infrared region," Phys. Rev. A, **43**,5597(1991).
2. Reuven Y. Rubinstein, Simulation and the Monte Carlo Method, Wiley, New York, 1981.
3. C. Wang, "Concise expression of a classical radiation spectrum," Phys. Rev. E, **47**(6)4358 (1993).
4. Ronald N. Bracewell, The Fourier Transform and Its Applications, 2nd ed. Mc Graw-Hill, Inc., 1986.
5. C. Wang and D. Xian, "RADID: software for insertion device radiation calculation," Nucl. Instr. and Meth. **A288**(1990)649.
6. J. Jackson, Classical Electrodynamics, chap.14, 2nd ed. Wiley, New York, 1975.
7. M. Born & E. Wolf, Principles of Optics, P317, 6th ed., Pergamon Press Inc, New York, 1980.
8. B.R. Frieden, "Computational methods of probability and statistics," in the Computer in Optical Research, edited by B.R. Frieden, Springer-Verlag, New York 1980.
9. S.O. Rice, in Selected Papers on Noise and Stochastic Processes, N. Wax ed., Dover publication, 1954.
10. J.W. Goodman, Statistical Optics, Wiley, New York, 1985.
11. K. J. Kim, "Characteristic of synchrotron radiation," in Physics of Particle Accelerators, M. Month & M. Dienes ed., AIP Conference proceedings **184**, vol.1 (1989) 565.
12. V. Ya. Epp and G.K. Razina, "Radiation in a wiggler with sinusoidal magnetic field," Nucl. Instr. and Meth. A**307**(1991)562.
13. R.P. Walker, "Near field effects in off-axis undulator radiation," Nucl. Instr. and Meth. A**267**(1988)537.
14. C. Wang and Y. Xiao, "On algorithms for undulator radiation calculation," in Proceedings of the International Conference on Synchrotron Radiation Sources, Indore, India, 1992. S.S. Ramamurthi, G. Singh, and D. Angal ed.
15. S. Marks, et at., "Insertion device magnet measurements for ALS," IEEE Particle Accelarator Conference, May 1993.
16. C. Wang, S. Marks, and B. Kincaid, "Spectral quality of ALS U5.0 undulator and field error effects," idem.
17. R.P. Walker and B. Diviacco, "URGENT--a computer program for calculating undulator radiation spectral,..." Rev. Sci. Instrum. **63**(1),1992.

LAWRENCE BERKELEY LABORATORY
UNIVERSITY OF CALIFORNIA
TECHNICAL INFORMATION DEPARTMENT
BERKELEY, CALIFORNIA 94720

ABH487
LBL Libraries